

Engineering Conferences International ECI Digital Archives

10th International Conference on Circulating
Fluidized Beds and Fluidization Technology -
CFB-10

Refereed Proceedings

Spring 5-2-2011

Flow Field in a Novel Short Residence Time Gas- solid Separator

Mengxi Liu

Chinese University of Petroleum (Beijing), mengxiliu@sina.com

Chunxi Lu

Chinese University of Petroleum (Beijing), lcxing@cup.edu.cn

Zhuan Wang

Chinese University of Petroleum (Beijing)

Follow this and additional works at: <http://dc.engconfintl.org/cfb10>

 Part of the [Chemical Engineering Commons](http://dc.engconfintl.org/cfb10)

Recommended Citation

Mengxi Liu, Chunxi Lu, and Zhuan Wang, "Flow Field in a Novel Short Residence Time Gas-solid Separator" in "10th International Conference on Circulating Fluidized Beds and Fluidization Technology - CFB-10", T. Knowlton, PSRI Eds, ECI Symposium Series, (2013). <http://dc.engconfintl.org/cfb10/11>

This Conference Proceeding is brought to you for free and open access by the Refereed Proceedings at ECI Digital Archives. It has been accepted for inclusion in 10th International Conference on Circulating Fluidized Beds and Fluidization Technology - CFB-10 by an authorized administrator of ECI Digital Archives. For more information, please contact franco@bepress.com.

FLOW FIELD IN A NOVEL SHORT RESIDENCE TIME GAS-SOLID SEPARATOR

Mengxi Liu, Chan Zhou, Chunxi Lu, Zhuan Wang
State Key Laboratory of Heavy Oil Processing
Faculty of Chemical Engineering, China University of Petroleum, Beijing,
Changping, Beijing, P.R.China, 102249
T: 0-8610-89733803; F: 0-8610-89733803; E: mengxi.liu@yahoo.com

ABSTRACT

The gas flow field in a short residence time separator was investigated. The tangential velocity in the separator housing increases with increasing angle to the positive x axis, and decreases with increasing radial position. A swirl of opposite direction to the main current in the separator housing occurs in the gas outlet.

INTRODUCTION

Gas-particle separators play a key role in a gas-solid fluidized bed by effectively collecting and recycling particles. Over the years, collection efficiency and pressure drop have been considered as the most important characteristics of a gas-particle separator (1-3). However, more concerns should be made when a separator is employed in a specific industrial process in which the reaction time is elaborately controlled, such as in the fluid catalytic cracking (FCC) process. Preferably, catalytic cracking reactions only occur in the riser reactor, which usually takes 1 to 5 s (4). Further contact of the highly active cracking catalysts and the cracked hydrocarbon vapor in the separator and the dilute phase is harmful, causing unwanted side reactions and byproducts (5-6). The catalysts are separated from the vapor at the end of the riser reactor, and the post riser reactor residence time is critically restricted. This is defined as the time the cracked hydrocarbon product remains in the separators and the dilute phase. A conventional scheme consists of multiple stage separators, usually a riser termination device and a cyclone. It provides high efficiency gas-solid separation, but allows a long and uncontrolled hydrocarbon post-riser residence time of 15-45 s in the separators and the reactor dilute phase, which significantly exceeds the time required by catalytic cracking reactions (4). Work associated with reducing post-riser residence time has been rare, mainly focused on the reduction in residence time in the separators and in the reactor dilute phase.

Gas-solid separators can be roughly categorized into centrifugal separators and inertial separators. A common and traditional centrifugal separator is the cyclone, which provides high separation efficiency, but allows relatively long contact time of gas and particles. Typical inertial separators are T-type ballistic riser terminators, which offer rough separation efficiency of approximately 60%. Recently, some novel short residence time separators (SRTS) have been proposed. Donsí *et al* (7)

presented a horizontally placed inertial riser terminator with a U-bend channel. Pictures and video show a particle-rich layer occurring within the first 60° of the separator circumference, indicating a rough separation of the gas-particle suspension. With increasing inlet gas velocity, the collection efficiency approximately remains constant (nearly 100%) for the high mass flow rate ranging from 260 to 340 kg/m²·s, but significantly decreases for the low mass flow rate less than 90 kg/m²·s. The retention time of the separation is only 4 ms. Andreus *et al* (4) presented a horizontal short contact time separator. In the separator, the gas-particle is centrifuged in a half-turn elbow, with particles moving downwards through the dipleg and gas exiting from a gas outlet horizontally located on the center of the separator head. Results show that the particle collection efficiency increases with increasing inlet solid loading and reaches an asymptotic value close to 95%. Variation of the back pressure exerted on the outlet of the dipleg has a slight influence on the particle collection efficiency, but a significant effect on the gas collection efficiency. A modified cyclone model was employed for prediction of the particle collection efficiency. Letzsch *et al* (5) and Joseph *et al* (6) proposed a novel separator called a rams horn, which combines centrifugal with inertial separations. The ram horn separator contains an upward flowing suspension inlet, a downward flowing solids outlet, a horizontally flowing gas outlet and a semi-circular separator area. The gas outlet extends through the separator housing and contains a horizontally disposed gas opening. Gas-solid suspension enters the SRTS vertically upwards and is then centrifuged in a half-turn elbow. Particles segregate at the concave wall of the separator housing and move vertically downward from the solid outlet, while the gas is withdrawn through gas openings on the gas outlet. The ram horn separator provides a number of significant potential advantages: small size, simple configuration, high collection efficiency, low pressure drop and short gas residence time. This work evaluates a novel ram horn-type short residence time separator with multiple gas openings uniformly disposed on the gas outlet.

MODEL DESCRIPTION

Mathematic Models

The flow field in a SRTS is characterized by a strongly swirling flow and anisotropic turbulence. The k - ε model, algebraic stress model (ASM) and Reynolds stress model (RSM) have been commonly employed in flow field simulation, but the RSM provides a more precise estimation on the strongly swirling flow and anisotropic turbulence (1). The governing equations of the continuous phase can be written as

$$\frac{\partial}{\partial t}(\rho\varphi) + \frac{\partial}{\partial x_j}(\rho u_j \varphi) = \frac{\partial}{\partial x_j}(\Gamma_\varphi \frac{\partial \varphi}{\partial x_j}) + S_\varphi \quad (1)$$

where φ is a universal variable, Γ_φ is the transport coefficient, S_φ is the source item. The expression of φ , Γ_φ and S_φ in different equations is listed in Table 1, where $\sigma_k=0.82$ and $\sigma_\varepsilon=1$. The inlet boundary was set as the uniform velocity inlet, and the turbulence quantities were also uniformly imposed on the inlet by using the correlations: $k_{in}=3/2(u_{in}l)^2$, and $\varepsilon_{in}=C_\mu^{0.75}k^{1.5}/l$, where $l=0.05$, $C_\mu=0.09$, $l=0.07 D_H$, and $D_H=0.108$ m. The boundary condition at the gas outlet was based on the fully developed flow assumption where the gradients of all variables in the flowing direction were taken to be zero. No-slip conditions were assumed at the wall.

Table 1 Governing equations of the CFD model

Equations	φ	Γ_φ	S_φ
Continuity equation	1	0	0
Momentum equation	u_i	μ	$-\frac{\partial p}{\partial x_i} + \frac{\partial(\frac{\mu \partial u_j}{\partial x_i})}{\partial x_j} + \rho g_i - \frac{\partial(\overline{\rho u_i' u_j'})}{\partial x_j}$
Turbulence dissipation equation	ε	$\mu + \mu_t / \sigma_\varepsilon$	$\varepsilon(c_{\varepsilon 1} P_{ij} / 2 - c_{\varepsilon 2} \rho \varepsilon) / k$
Reynolds stress equation	$\overline{u_i' u_j'}$	$\mu + \mu_t / \sigma_k$	$P_{ij} + \varepsilon_{ij} + \phi_j$

Geometric Model

The inlet gas velocity is set as 16.12 m/s. The schematic diagram and structured mesh of the SRTS is shown in Fig. 1. It is seen that the SRTS contains a semi-circular separator housing which is connected with an inlet of upward flowing gas-solid suspension and a downward flowing solid outlet or dipleg. A 156 mm ID gas outlet is horizontally and centrally located, extending through the separator housing and paralleling the base of the separator and the inner concave surface of the separator housing. Several horizontal gas openings are disposed uniformly around the gas outlet. The width of the inlet and outlet is 68 mm and 73 mm, respectively. The radius of the concave surface and the width of the separator housing is 157.5 mm and 268 mm. Coordinate directions of x, y, z are illuminated in Fig.1.

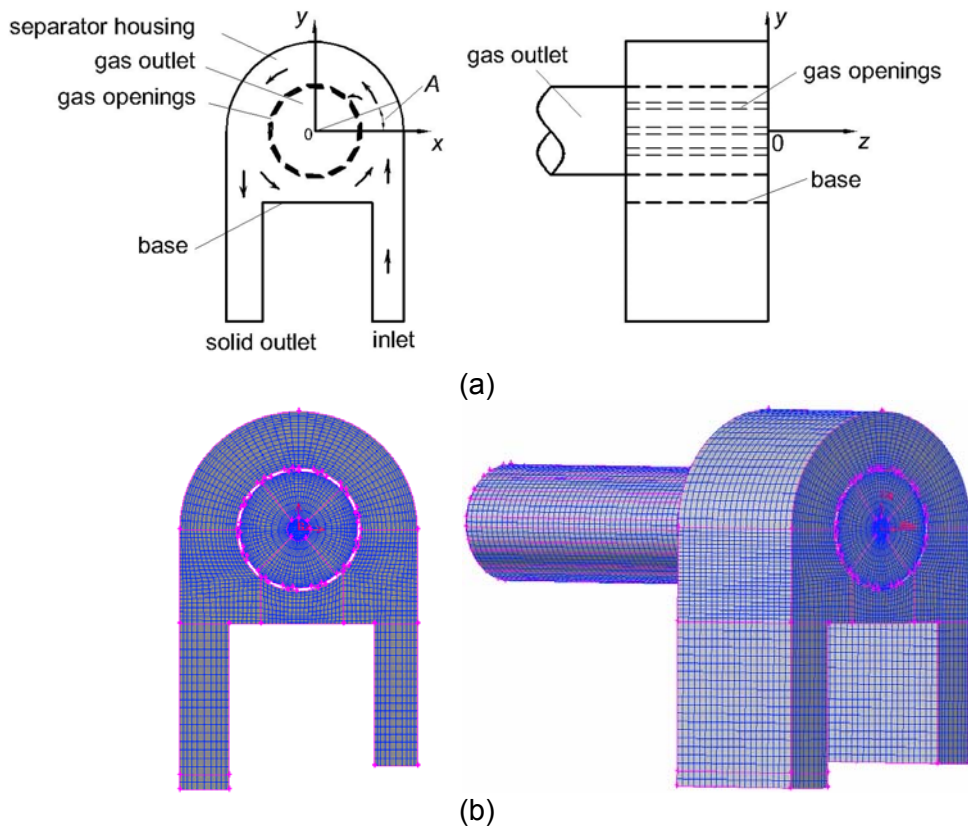


Fig.1 Schematic diagram and structured mesh of the SRTS

Model Validation

In order to validate the CFD simulation method described above, the predicted results were compared with available experimental data obtained in a cold model SRTS having the same size. Fig.2 shows that data from both methods are close, indicating validation of the established CFD models.

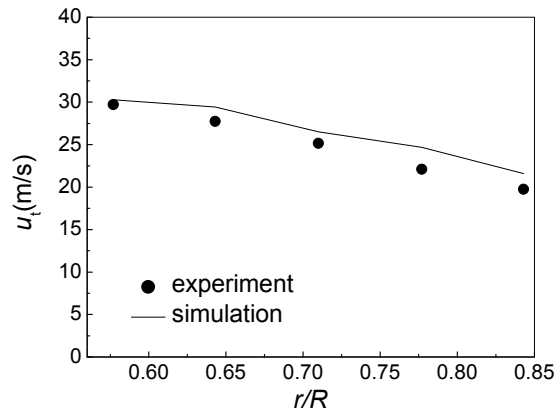


Fig. 2 Comparison of results from experiment and simulation

RESULTS AND DISCUSSION

Flow Field in Separator Housing

Fig.3 gives the velocity vectors on the vertical plane of $z = 100$ mm of SRTS. In the range of $0^\circ < A < 180^\circ$, the gas velocity is always higher than the inlet gas velocity, indicating a greater gas flow rate in the SRTS. As shown in Fig. 1, the gas flow in the SRTS can be categorized into two types: gas flow entering the gas outlet through the gas openings and gas flow circulating in the separator housing. The latter significantly increases the gas flow rate in the separator housing, leading to a greater gas velocity than in the inlet. Moreover, the gas velocity in the bottom region, the space between the gas outlet and the base, is large, mainly arising from the decrease of the cross-sectional area.

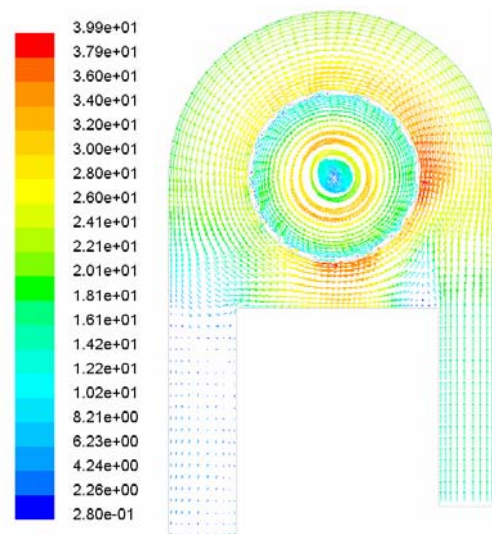


Fig.3 Velocity vectors on the plane of $z = 100$ mm

The tangential gas velocity governs the centrifugal force and the particle collection. Fig. 4 shows the variation of tangential gas velocity as a function of dimensionless radial position and A , the angle to the positive x axial as shown in Fig. 1. It is seen that the tangential gas velocity decreases with increasing radial position, with the maximum near the outer surface of the gas outlet and the minimum at the vicinity of the inner concave surface of the separator housing. The tangential gas velocity also varies along the circumference. As shown in Fig. 4, the tangential velocity decreases as A increases, arising from the decrease of the gas flow rate and leading to decreasing centrifugal force.

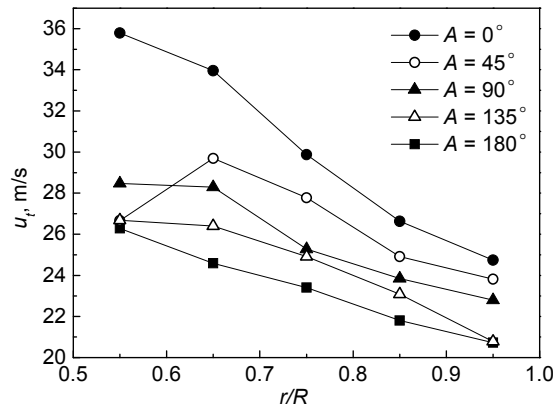


Fig. 4 Variation of tangential gas velocity as a function of radial position and A

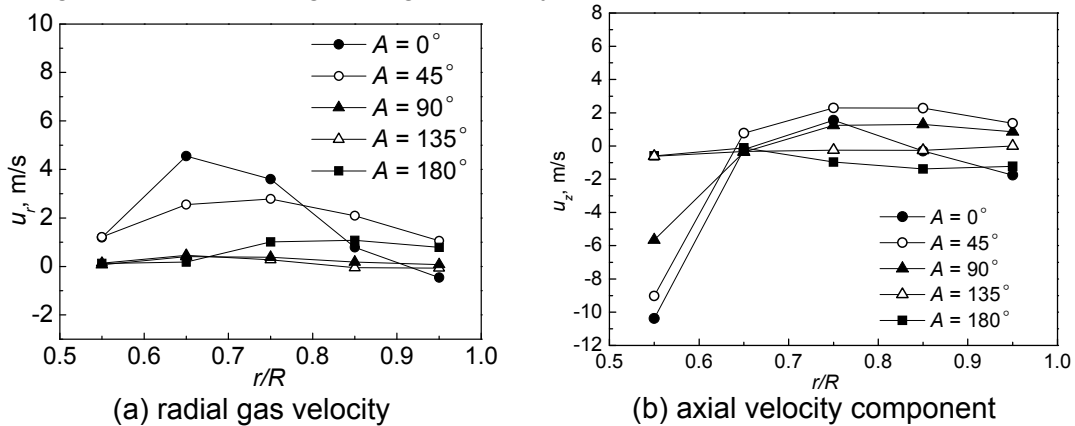


Fig. 5 Variation of radial and axial velocity components as a function of radial position and A

Fig. 5 presents the variation of radial and axial velocity components as a function of radial position and A . In this work, the radial velocity in the direction opposite to the centrifugal force is defined to be positive. It is seen that the radial velocity decreases with increasing A within the first 45° of the separator circumference, while it is approximately zero when A is greater than 45° . The axial velocity does not show a regular variation, except that it is negative at the vicinity of the gas outlet ($r/R=0.495$), probably influenced by the gas flow in the gas outlet which also has a negative axial velocity.

Flow Field in the Bottom Region

As discussed before, gas not only enters the gas outlet through the gas openings, but also circulates in the separator housing. The variation of the cross-sectional area

of the bottom region governs the circulation gas flow rate and influences the pressure drop of the SRTS, while the former significantly increases the gas flow rate in the SRTS and affects the particle collection efficiency. Fig. 6 shows the tangential gas velocity in the bottom region. When gas passes through the bottom region, the tangential velocity increases first, reaches the maximum when x is close to 0, and then decreases. This is dominated by the variation of the cross-sectional area of the bottom region, with a contraction for $x < 0$ and an enlargement for $x > 0$ (Fig. 1). Fig. 6 shows that the tangential velocity also changes with the distance to the gas outlet. The closer to the gas outlet, the higher the tangential velocity. This is similar to the variation of the tangential velocity for $0^\circ < A < 180^\circ$.

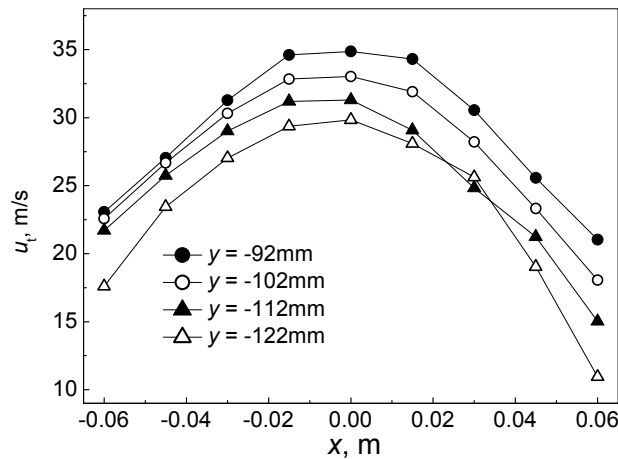


Fig. 6 Variation of the tangential velocity in the bottom region

Fig.7 (a) presents the profile of the radial velocity in the bottom region. It is seen that the radial velocity increases with increasing x , with consistently negative values for $x < 0$, which is probably caused by inertial force, and positive velocity for $x > 0$. Moreover, the radial velocity increases with height. The axial velocity seems to be almost constant along the x axis, Fig.7(b).

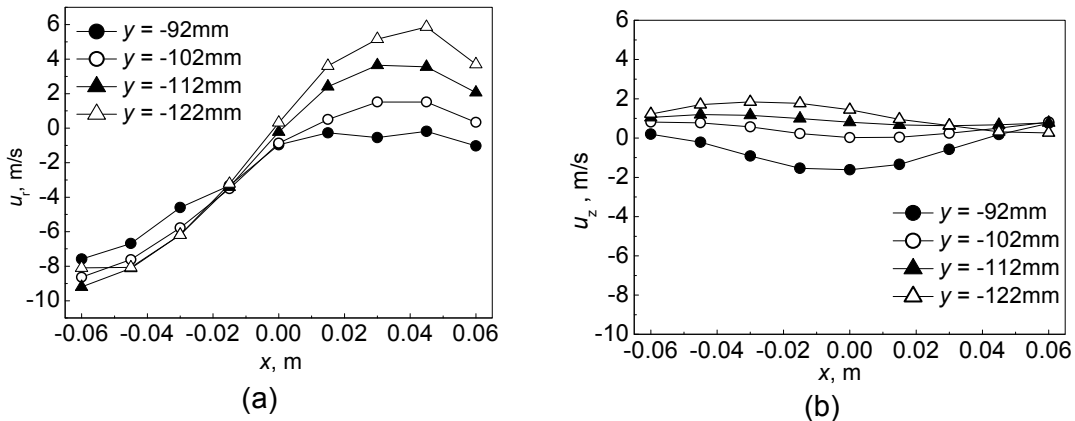


Fig. 7 Variation of the radial and axial velocities in the bottom region

Flow Field in the Gas Outlet

Fig. 8 presents the tangential velocity variation in the gas outlet. It is seen that the tangential velocity is consistently negative, indicating a clockwise swirling flow occurring in the gas outlet. Gas openings were initially made with slanting edges.

These slanting edges lead to a sharp turn when the gas-particle suspension enters the gas openings. In this way, particles are separated by inertial force. The tangential velocities are close to each other for different A , signifying that every gas opening on the gas outlet gets approximately the same gas flow rate. Moreover, the tangential velocity is very small for r/R close to zero, mainly caused by the eddy at the center of the gas outlet.

The axial gas velocity at different cross sections of the gas outlet is shown in Fig. 9. It is seen that the axial velocity near the wall of the gas outlet is greater than that at the center. There is a big difference in the axial velocity between the cross sections of $z=100$ mm and 200 mm, signifying a spiral motion in the gas outlet. Moreover, the evolution of the axial velocity along the radial direction at the cross-section of $z=600$ mm is more fluent than that of $z=100$ mm and 200 mm, signifying a fully developed flow near the exit of the gas outlet.

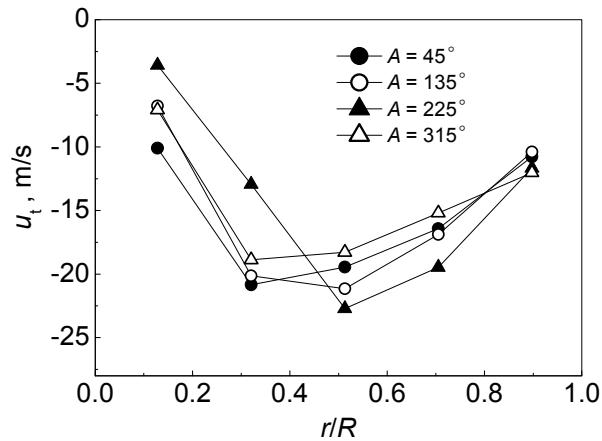


Fig. 8 Tangential velocity in the gas outlet

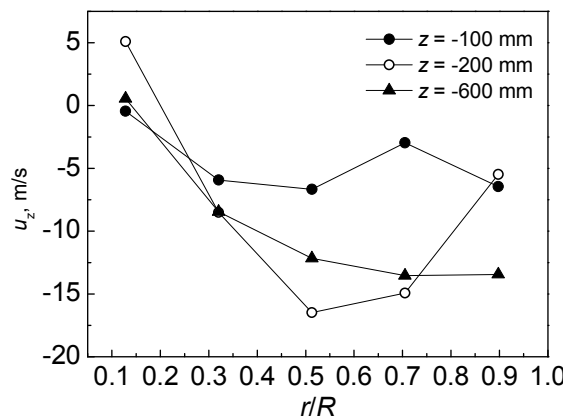


Fig. 9 Axial velocity at different cross-sections of gas outlet

CONCLUSION

The flow field in a novel ram horn-type short residence time separator (SRTS) was investigated by CFD simulation. The gas flow rate in the SRTS is significantly greater than the feed flow rate. The tangential velocity in the separator housing increases

with the increase of the angle to the positive x axis, and decreases with increasing radial position. The radial velocity is positive at the vicinity of $A=0^\circ$, but approximately equals zero in the remaining regions. Influenced by the gas flow in the gas outlet, the axial velocity is negative at the vicinity of the gas outlet ($r/R=0.495$). In the bottom region, the tangential velocity is governed by the cross-sectional area of the region. The radial velocity increases with increasing x , being negative for $x<0$ and positive for $x>0$. Because of the slanting edges of the gas openings, the gas passing through the gas openings in the reverse direction, and a swirl in the opposite swirling direction to the main flow in the separator housing occurs in the gas outlet.

NOTATION

A	angle of the gas opening to positive x axis, $^\circ$
D_H	hydrodynamic diameter, m
k	turbulent kinetic energy
l	turbulence intensity
S_φ	source item of equation (1)
u_r	radial velocity, m/s
u_t	tangential velocity, m/s
u_z	axial velocity, m/s
x	x axis as shown in Fig.1
<i>Greek letters</i>	
φ	universal variable, -
Γ_φ	transport coefficient, -
ρ	density, kg/m^3
μ	viscosity, Pa.s
σ_k	Prandtl number of turbulent kinetic energy k
σ_ε	Prandtl number of turbulent dissipation rate ε
ε	turbulent dissipation rate, m^2/s^3

REFERENCES

1. G. Wan, G. Sun, X. Xue, M. Shi. Solids concentration simulation of different size particles in a cyclone separator. *Powder Technol.*, 183 (2008), 94-104.
2. L. Shi, D.J. Bayless. Comparison of boundary conditions for predicting the collection efficiency of cyclones. *Powder Technol.*, 173 (2007), 29-37.
3. F. Kaya, I. Karagoz. Numerical investigation of performance characteristics of a cyclone prolonged with a dipleg. *Chem. Eng. J.* 151 (2009), 39-45.
4. R. Andreux, G. Ferschneider, M. Hémati, O. Simonin. Experimental study of a fast gas-particle separator. *Chem. Eng. Res. and Des.* 85(6) (2007), 808-814.
5. W. S. Letzsch, G. Earl. Short residence time cracking apparatus and process. U.S. Patent 5, 662, 868, Sep. 2, 1997
6. J.L. Ross, Jr., C.S. Caty, C.J. Horecky. Apparatus for separating fluidized cracking catalysts from hydrocarbon vapor. U.S. Patent 5, 259, 855. Nov. 9, 1993.
7. G. Donsì, L.S. Osséo, M. Schenato. Experimental characterization of a short retention time gas-solid separator. *Powder Technol.*, 85 (1995), 11-17.